Changes in mineral reactivity driven by pore fluid mobility in partially wetted porous media

A.L. Harrison[a,*,1], G.M. Dipple[a], W. Song[b], I.M. Power[a], K.U. Mayer[a], A. Beinlich[a,c], D. Sinton[b]

[a] Department of Earth, Ocean and Atmospheric Sciences, The University of British Columbia, 2207 Main Mall, Vancouver, British Columbia V6T 1Z4, Canada
[b] Department of Mechanical and Industrial Engineering and Institute for Sustainable Energy, University of Toronto, 5 King's College Road, Toronto, Ontario M5S 3G8, Canada
[c] The Institute for Geoscience Research (TIGeR), Curtin University, 6845 Perth, Australia

ARTICLE INFO

ABSTRACT

Microfluidics experiments were used to examine mineral dissolution-precipitation reactions under evaporative conditions and identify pore-scale processes that control reaction rate. The entrainment of reacting mineral particles by a mobile water-gas interface driven by evaporation dramatically altered the relative abundance of reactive mineral surface area to fluid reservoir volume. This ratio, which directly influences reaction rate and reaction progress, was observed to vary by nearly two orders of magnitude as evaporation progressed in the experiments. Its dynamic evolution may have a correspondingly large impact on mineral-fluid reaction in Earth's shallow subsurface. We predict that the spatial and temporal variability of pore-scale reaction rates will be significant during evaporation, imbibition, or drainage in the vadose zone, with implications for chemical weathering, soil quality, and carbon cycling. Variable reaction rates during particle mobility are likely to be of increased significance as global rainfall patterns and soil moisture contents evolve in response to climate change.

1. Introduction

Mineral-fluid reactions in Earth's shallow subsurface regulate element transport in nature, disturbed environments, and human-made materials such as industrial wastes. They are vital for nutrient availability, water quality, and carbon cycling (Blowes and Jambor, 1990; Brantley and White, 2009; Maher et al., 2009; Manning, 2008; McKinley et al., 2006). Despite the importance of mineral-fluid reactions in controlling element cycling, predictions of large-scale mass transport are hindered by the scale-dependence of mineral dissolution-precipitation rates and the use of the continuum approach in numerical models that represents porous media with continuous domains of volume-averaged properties (Molins et al., 2012). This approach can lead to significant error in the prediction of geochemical reaction rates (Li et al., 2008, 2006; Molins et al., 2012). As global patterns in rainfall and soil moisture content evolve in response to climate change (IPCC, 2013), the impact of wetting and drying on mineral-fluid reactions is likely to be of increased significance and concern. In particular, unsaturated porous media exhibit highly heterogeneous pore micro-environments that are subject to significant change during gas and fluid mobility. Others have posited that particle entrainment by the mobile fluid meniscus during evaporation or water recharge contributes to hardening of soils, and have shown indirect textural evidence of this process (Bresson and Moran, 1995; Mullins et al., 1987), and Shahidzadeh et al. (2015) demonstrate entrainment of freshly precipitated salt crystals by the retreating air-water interface during unconstrained droplet evaporation. Yet, the chemical impacts of such particle mobility in porous media have not been assessed. We anticipate that pore-scale reaction rates will be highly dynamic and variable in these environments, potentially altering net chemical fluxes derived from dissolution reactions in porous media, and resulting in heterogeneous distribution of secondary phases.

Experiments using microfluidic reactors (i.e., micromodels) allow visualization of pore-scale processes that can inform development of pore-scale reactive transport models (Boyd et al., 2014; Yoon et al., 2012). To date, most of these experiments have focused on flow dynamics. Only recently have mineral precipitation reactions been studied in water-filled micromodels (Boyd et al., 2014; Yoon et al., 2012; Zhang, 2010) and very few have investigated precipitation in mixed fluid-gas conditions representative of the shallow subsurface (Kim et al., 2013). Here, we consider the reactivity of magnesium hydroxide in the form of the mineral brucite [Mg(OH)$_2$], of interest

* Corresponding author.
  E-mail addresses: anna.harrison@ucl.ac.uk (A.L. Harrison), gdipple@eoas.ubc.ca (G.M. Dipple), wensong@stanford.edu (W. Song), ipower@eoas.ubc.ca (I.M. Power), umayer@eoas.ubc.ca (K.U. Mayer), andreas.beinlich@curtin.edu.au (A. Beinlich), sinton@mie.utoronto.ca (D. Sinton).
  [1] Present address: Department of Earth Sciences, University College London, Gower Street, London WC1E 6BT, UK.

because of its fast reaction rate at ambient laboratory conditions, because it actively reacts with the atmosphere to sequester carbon, and has recently drawn attention for its potential use for phosphorus recovery from wastewaters (Harrison et al., 2016, 2015, 2013; Hövelmann and Putnis, 2016; Hövelmann et al., 2012; Power et al., 2013; Ulven et al., 2017). We investigated coupled brucite dissolution-carbonate mineral precipitation in a variably water-filled glass micromodel under evaporative conditions to elucidate controls on mineral-fluid reactions and highlight the importance of pore-scale processes on reactivity at conditions representative of the shallow, variably saturated, subsurface.

2. Methods

2.1. Experimental methods

As an example of coupled mineral dissolution-precipitation reactions in the shallow subsurface, duplicate microfluidic brucite carbonation experiments were conducted using an unsaturated silica glass micromodel. Although brucite is not an abundant mineral at the Earth's surface, its rapid reaction rates make it an ideal candidate to observe coupled dissolution-precipitation reactions on an experimental timescale, and it can be utilized to sequester atmospheric CO_2 (Assima et al., 2012; Harrison et al., 2015; Hövelmann et al., 2012; Zhao et al., 2010). The micromodel had a pore network that was 5.0 cm long by 1.5 cm wide with cylindrical glass pillars representative of quartz [SiO_2] grains (Fig. 1). The network consisted of regularly spaced pillars of two sizes: ~180 μm and ~70 μm. Pore throats were between ~215 and 260 μm, the depth was ~130 μm, and the porosity was approximately 0.87. The micromodel was fabricated using standard photolithography techniques and wet etching with hydrofluoric acid (Kim et al., 2013). Prior to experimentation and between experiments, the micromodel was thoroughly flushed with toluene, isopropyl alcohol, 12 M hydrochloric acid, deionized water, and then the experimental slurry. Experimental slurries consisted of 0.5 M $MgCl_2$ prepared using deionized water and reagent grade $MgCl_2 \cdot 6H_2O$, and 5 wt% pulverized brucite. Slurries were sonicated to minimize particle aggregation prior to injection into the micromodel with a syringe (Song and Kovscek, 2015).

After the slurry was injected, multiple pore volumes of research grade gaseous CO_2 (99.99% purity; Praxair) were flushed through the micromodel to partially displace the slurry, leaving the pore network with variable water and brucite content (i.e., not all pores were filled with slurry). The micromodel was then immediately connected to a stream of 99.99% purity CO_2 supplied at a constant flow rate of 0.5 mL min^{-1} using a Teledyne ISCO model D-260 pump. A high CO_2 supply rate (0.5 mL min^{-1}) compared to the micromodel pore volume (~85 μL) was utilized to ensure that the carbonation reaction was not limited by a lack of CO_2. The first experiment was conducted for 18 h, and the second for 8 h.

Time lapse greyscale brightfield images were taken at 5 min intervals during the experiment using an inverted Olympus CKX41

transmitted light microscope (250 × objective) and an Orca-ER Hamamatsu camera with resolution of 6.45 μm × 6.45 μm per pixel. ImageJ (Abràmoff et al., 2004) software was used to compile these images into video format (Supporting Information (SI) Videos S1 and S2) at 2 frames per second (approximately 10 min of experiment time to 1 s of video). Videos S1 and S2 are a compilation of images collected during the 8 h and 18 h experiment, respectively. The field of view in Videos S1 and S2 are 3.4 mm × 2.2 mm and 1.9 mm × 1.3 mm, respectively. Only the first ~10 h of the latter are included, as little change was observed for the remainder of the experiment. Additional images were collected in color to characterize the entire pore network following the second experiment using a Nikon eclipse E600 POL microscope and Canon EOS Rebel T2i camera. Raman spectra of the reaction products were collected following the second experiment using a Renishaw inVia microscope with 785 nm excitation. Mineral identifications were conducted with reference to the RRUFF™ database of Raman spectra.

In addition to the micromodel experiments, an experiment was conducted to visualize the behavior of the brucite slurry under the influence of evaporation alone, without the carbonation reaction. In this experiment a brucite slurry of the same composition as that in the micromodels was constrained between two glass slides with its evaporation observed in real time using a Nikon eclipse E600 POL microscope. Photographs were taken periodically with a Canon EOS Rebel T2i camera. The slurry was confined vertically between two glass slides but remained open to the air at the edges of the slides to permit evaporation.

2.2. Characterization and preparation of initial brucite slurry

The brucite was obtained from Premier Magnesia LLC, and was pulverized using a hammermill and subsequently sieved to ≤ 53 μm in diameter. The particle size distribution was determined using a Malvern Mastersizer 2000 Laser Diffraction Particle Size Analyzer, which indicated that the mean particle diameter was 23 μm. The initial surface area of duplicate samples was determined by multipoint BET with N_2 adsorption using a Quantachrome Autosorb-1 surface area analyzer. It was equal to 5.2 ± 0.2 m^2 g^{-1}.

Rietveld refinement of X-ray diffraction (XRD) data was used to quantify the initial mineralogical composition of the brucite. Triplicate samples were spiked with 10 wt% highly crystalline CaF_2 to allow quantification of the amorphous (non-crystalline) content (Gualtieri, 2000; Wilson et al., 2006). Samples were ground under ethanol for 5 min using a McCrone micronizing mill and agate grinding elements to reduce the mean particle size. Micronized samples were gently disaggregated with an agate mortar and pestle when dry. The samples were placed in back-loaded cavity mounts against sandpaper to minimize preferred orientation (Raudsepp and Pani, 2003). A Bruker D8 Focus Bragg-Brentano diffractometer with CoKα radiation and a step size of 0.04° over a range of 3–80°2θ at 0.09 s/step was employed. The long fine focus Co X-ray tube was operated using a take-off angle of 6°at
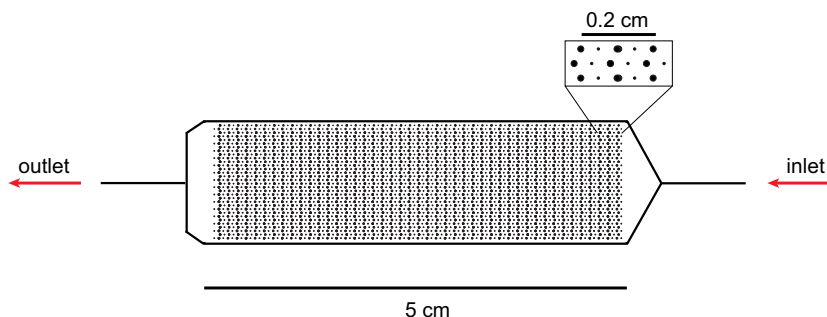

Fig. 1. Schematic of the micromodel pore network. The inset figure illustrates the arrangement of the cylindrical glass pillars in three dimensions, which extended over the entire (~130 μm) depth of the micromodel.